3D Phase Unwrapping Based on Expansion in Chebyshev Polynomials

J. Langley[1,2], and Q. Zhao[1,2]

[1]Physics and Astronomy, The University of Georgia, Athens, GA, United States, [2]Bioimaging Research Center, The University of Georgia, Athens, GA, United States

Introduction

In MR images, phase contains information about magnetic field inhomogeneities and the chemical shift of tissues. Phase is only defined on the principal interval. The principal interval has a range of $(-\pi,\pi]$. When phase falls outside the principal interval, integer values of 2π are added to the phase until it falls within the principal interval. This process is known as phase wrapping. Areas of MR where phase unwrapping plays a key role include: susceptibility weighted imaging, correction of geometric distortions in diffusion tensor imaging and echo-planar imaging, and venography. Additionally, phase can be used to indirectly detect the presence of superparamagnetic iron oxide (SPIO) nanoparticles. The phase gradient mapping method (PGM) is able to locate the distribution of SPIO nanoparticles by using the susceptibility gradients created by the SPIO nanoparticles. Higher concentrations of SPIO nanoparticles will create larger susceptibility gradients. The PGM method calculates the susceptibility gradients caused by SPIO nanoparticles from phase gradients. Most of the previously proposed phase unwrapping algorithms are inherently two dimensional. Applying a 2D phase unwrapping algorithm to a 3D data set and unwrapping individual slices causes discontinuities in phase between slices in the unwrapped 3D phase map. In this abstract, this problem is solved by extending the phase unwrapping algorithm introduced in [1] into three dimensions. The phase unwrapping algorthim is applied to the PGM method.

Theory and Methods

Previous work has shown that a 2D MR phase map can be modeled as a product of 1D Chebyshev polynomials of the first kind [1]. We extend that phase unwrapping procedure to 3D by assuming the phase in a 3D MR phase map can be modeled as a product of three 1D Chebyshev polynomials of the first kind

$$\varphi(x,y,z)=\sum_{n=0}^{N}\sum_{m=0}^{n}\sum_{r=0}^{m}a(n,m,r)T_{n-m}(x)T_{m-r}(y)T_r(z)-r(x,y,z) \tag{1}$$

where N is the expansion order, $T_i(x)$ are Chebyshev polynomials of the first kind, $a(n,m,r)$ are expansion coefficients, and $r(x,y,z)$ is the remainder function. The phase can be modeled as a product of three 1D Chebyshev polynomials provided the phase map is piecewise continuous. The remainder function covers all expansion terms higher than the expansion order. We can easily solve for $a(n,m,r)$ by exploiting orthogonality of Chebyshev polynomials on the interval [-1,1]. Computing the partial derivative of (1) with respect to x and using the orthogonality of both types of Chebyshev polynomials on the interval [-1,1] gives

$$a^x(n,m,r)=\frac{1}{n-m}\left(\frac{2^{3-\alpha-\beta}}{\pi^3}\right)\int_{-1}^{1}\int_{-1}^{1}\int_{-1}^{1}d^3x\;\frac{U_{n-m-1}(x)T_{m-r}(y)T_r(z)\sqrt{1-x^2}}{\sqrt{1-y^2}\sqrt{1-z^2}}\frac{\partial\varphi}{\partial x} \tag{2}$$

where $\alpha=\delta_{mr}$, $\beta=\delta_{r0}$, and δ_{mn} is the discrete Kronecker delta function. Following similar procedures allows for the calculation of the expansion coefficients associated with the other two partial derivatives along *y and z*. The total expansion coefficients are calculated by averaging the expansion coefficients calculated from the partial derivatives. The remainder function is defined to be

$$r(x,y,z)=\mathrm{Arg}\;\exp\left(i\left\{\sum_{n=0}^{N}\sum_{m=0}^{n}\sum_{r=0}^{m}a(n,m,r)T_{n-m}(x)T_{m-r}(y)T_r(z)-\varphi(x,y,z)\right\}\right) \tag{3}$$

where Arg x returns the principal value of x.

Results and Discussion

The 3D phase unwrapping algorithm was applied to the phase maps from two datasets. The first dataset was acquired from a human subject's brain. The phase map was acquired on a 3.0 T GE Signa HDX MR Scanner (GE Medical Systems, Milwaukee, WI) using a 3D fast gradient echo pulse sequence (TE/TR = 2.2 / 5.6 ms, flip angle = 60 degrees, matrix size = 128 x 128). The second dataset was acquired from an agar phantom with three vials embedded within the phantom. SPIO nanoparticles were placed within each vial in the phantom. A fast gradient echo pulse sequence (TE/TR=7 /150 ms, flip angle = 90 degrees, matrix size=128 x 128) was used to acquire the phantom data set. The results of the phase unwrapping procedure are shown in Fig. 1 and 2 for the two datasets. An axial view of wrapped phase map from the brain is shown in Fig. 1a. The corresponding unwrapped phase map is shown in Fig. 1b. A sagittal view of the wrapped phase is displayed in Fig. 1c. The corresponding unwrapped phase map is shown in Fig. 1d. The 3D phase map was unwrapped with an expansion order of N = 15. The phase unwrapping algorithm applied to the phantom dataset is shown in Figure 2. The wrapped phase is shown in Fig. 2a and the corresponding phase gradient map calculated from the direct derivatives is shown in Fig. 2b. The unwrapped phase map is shown in Fig. 2c and the phase gradient map calculated from the direct derivatives is shown in Fig. 2d. The phase map was unwrapped using an expansion order of N = 14.

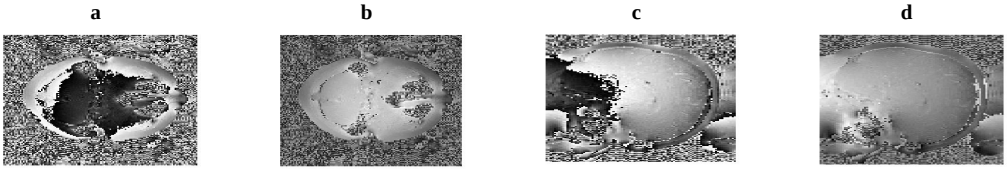

Figure 1. A: View of the wrapped phase map in the axial plane. B: Unwrapped phase map corresponding to the phase map in A. C: View of the wrapped phase map in the sagittal plane. D: Unwrapped phase map corresponding to the phase map in C.

As in [1], the remainder function is bound within the principal interval. Wrapping in the remainder function occurs when $r(x,y,z)$ falls outside the principal interval. Wrapped areas in the remainder function correspond to areas with a discontinuous jump of $\pm2\pi$ in the unwrapped phase map. Unwrapping the remainder function will mitigate this problem in most circumstances. Wrapping in the phase map is problematic for the PGM method because it generates false detections (indicated by red arrows in Fig. 2B) of the SPIOs in the PGM method. Unwrapping the phase map or calculating the phase gradients in k-space will mitigate the amount of false detections.

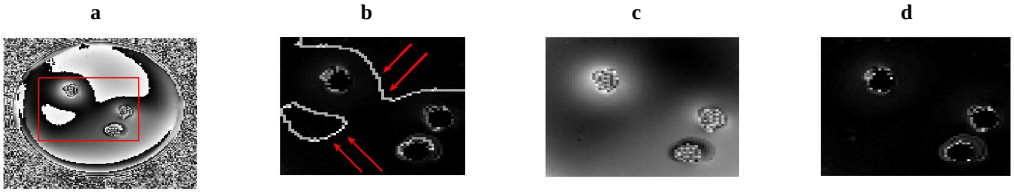

Figure 2. A: Wrapped phase map of the phantom. The box shows the ROI chosen for B-D. B: The PGM of the wrapped phase map in A. The red arrows indicate false detections due to wrapping. C: Unwrapped phase map of the phantom. D: The PGM of the phase map in C.

References: [1] Langley, J., Zhao, Q., *Proc. IEEE EMBC 2008*, p 4043-4046. [2] Liang, Z.P., *IEEE TMI*, 15,893-897,1996.

Acknowledgement: This study was supported by the University of Georgia Faculty Research Grant.